

# Excitons in long molecular chains near the reflecting interface

Yu. N. Gartstein<sup>1</sup> and V. M. Agranovich<sup>2,3</sup>

<sup>1</sup>*Department of Physics, The University of Texas at Dallas, Richardson, TX 75083, USA*

<sup>2</sup>*UTD-NanoTech Institute, The University of Texas at Dallas, Richardson, TX 75083, USA*

<sup>3</sup>*Institute of Spectroscopy, Russian Academy of Science, Troitsk, Moscow, Russia*

We discuss coherent exciton-polariton states in long molecular chains that are formed due to the interaction of molecular excitations with both vacuum photons and surface excitations of the neighboring reflecting substrate. The resonance coupling with surface plasmons (or surface polaritons) of the substrate can substantially contribute to the retarded intermolecular interactions leading to an efficient channel of the decay of one-dimensional excitons with small momenta via emission of surface excitations. The interface also modifies the radiative decay of excitons into vacuum photons. In an idealized system, excitons with higher momenta would not emit photons nor surface waves. For a dissipative substrate, additional exciton quenching takes place owing to Joule losses as the electric field of the exciton polarization penetrates the substrate. We discuss how these effects depend on the polarization of molecular excitations, their frequency and on the distance of the chain from the substrate.

PACS numbers: 78.67.-n, 71.35.Aa, 71.36.+c, 73.20.Mf

## I. INTRODUCTION.

The interaction of the electromagnetic field with a molecular excitation in an aggregate of identical molecules leads, on the one hand, to the delocalization of the excitation over the aggregate and, on the other hand, to a modification of its radiative decay.<sup>1</sup> Both notions of excitons and polaritons are used in the literature on such delocalized excitations. In crystalline structures, the excitation can be spatially coherent and then it is characterized by its wave vector as a proper quantum number. In this paper we discuss how electric-dipole-active coherent excitations in linear crystals are affected by the presence of a neighboring metallic/dielectric half-space.

A variety of one-dimensional (1D) electronic systems available nowadays, such as conjugated polymers,  $J$ - and  $H$ - aggregates, semiconducting quantum wires and carbon nanotubes, exhibit interesting optical properties and are considered for potential applications in optoelectronics; their spectroscopy is an active research area. Successes at the synthesis and fabrication of these systems have resulted in the continuously improving quality and the increase of their “conjugation length”  $L$  which may exceed the appropriate electromagnetic wave length  $\lambda$ . Perhaps one of the most noteworthy achievements in this regard is a recent observation<sup>2</sup> of a macroscopic coherence of a single exciton in polydiacetylene chains of  $L \simeq 10 \mu\text{m}$  that allowed to discuss an issue of “an ideal 1D quantum wire”.<sup>3</sup> It is also relevant to note a physically very different but conceptually related class of excitations in chains of “dipole-coupled” nanoparticles (see, e. g., a recent Ref. 4 and multiple references therein) studied for photonic and plasmonic applications.

Long before the modern experimental advances, it was shown<sup>1,5</sup> that the coherent interaction of low-dimensional (1D and 2D) excitons with the electromagnetic field is drastically different than in 3D systems. The radiative decay of low-dimensional excitons is strongly enhanced in

the region of their wave vectors  $|\mathbf{q}| \leq k$ , where  $k = \omega/c$  ( $c$  is the speed of light in vacuum) is determined self-consistently by the excitation energy  $E(\mathbf{q}) = \hbar\omega$ , while the excitations with  $|\mathbf{q}| > k$  would not radiate, as is required by the energy and momentum conservation for an exciton-photon system. More specifically, for 1D excitons in the molecular chain in vacuum, the radiative width  $\Gamma = \hbar/\tau$  ( $\tau$  being the decay time) depends on the wave vector  $q$  as

$$\Gamma^v(k, q) = \frac{\pi p^2}{a} [2(k^2 - q^2) \cos^2 \theta + (k^2 + q^2) \sin^2 \theta] \Theta(k - |q|), \quad (1)$$

where  $p$  is the magnitude of the molecular dipole transition moment  $\mathbf{p}$  that makes angle  $\theta$  with the chain axis,  $a$  the intermolecular spacing along the chain, and  $\Theta$  the step-function. As compared with the radiative width

$$\Gamma^0(k) = 4p^2 k^3 / 3 \quad (2)$$

of a single molecule, Eq. (1) exhibits an enhancement factor of  $\sim \lambda/a = 2\pi/ka \sim 10^2 - 10^3$  in the optical region of the spectrum (“superradiant” states). This enhancement has been discussed in the context of various systems (see, e. g., Refs. 6,7,8,9 and references therein). Equation (1) also shows how the polarization of the transition dipole affects the  $q$ -dependence of the decay rate.

Importantly for applications, it is possible to manipulate the optical properties of molecular excitations and to form new hybrid excitations by putting molecules or molecular aggregates in the vicinity of interfaces and in dielectric microcavities.<sup>10</sup> Well-known, e.g., is an oscillating dependence of the radiative width on the distance of a single molecule from the planar interface resulting from the interference of the radiative fields of a molecular transition and its image.<sup>10,11</sup> The dipole-dipole interaction gets also modified in the vicinity of a surface or in the cavity.<sup>12,13,14</sup> In the case of a linear molecular crystal, the environment can lead to qualitatively interesting

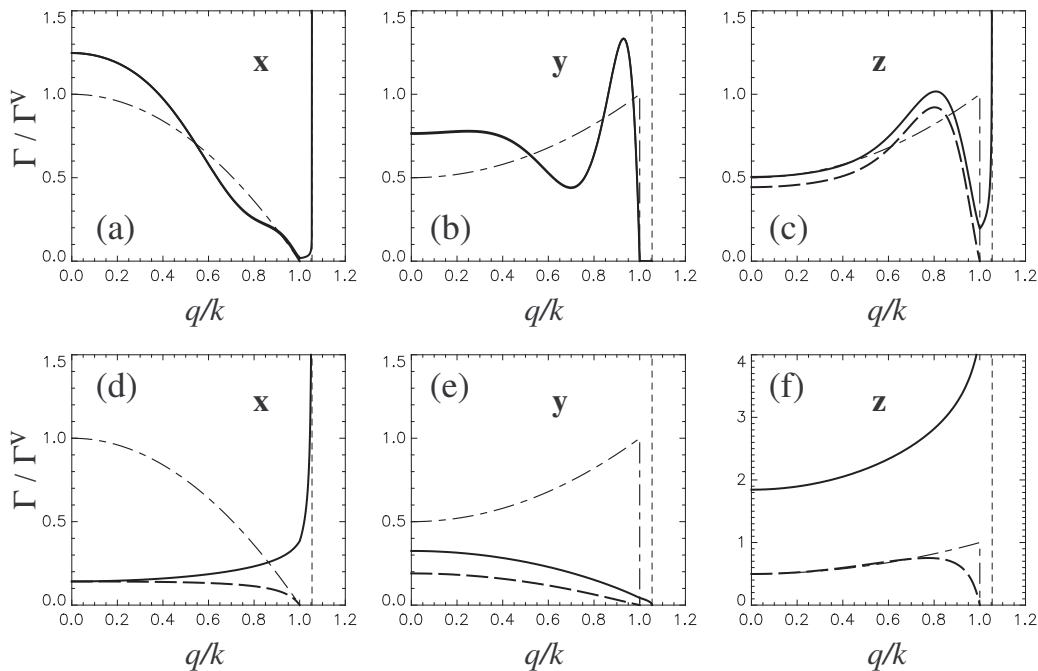


FIG. 1: Decay width  $\Gamma(k, q)$  of 1D exciton-polaritons as a function of the reduced wave vector  $q/k$  for a fixed value of  $k = 2\pi/400a$  and substrate's dielectric constant  $\epsilon = -10$ . Two rows correspond to different dipole-to-image-dipole distances  $d$ : upper panels (a-c) are for  $d = 600a$ , lower panels (d-f) for  $d = 10a$ . All distances are measured in units of intermolecular spacing in the chain,  $a$ . Each of the trio of the panels in a row corresponds to different exciton polarization, indicated by the boldface letters. The chain is parallel to the  $x$ -axis and situated above the substrate whose surface is the  $xy$ -plane. Decay width is shown with respect to  $\Gamma^v = 2\pi p^2 k^2/a$  which is the radiative width of the  $x$ -polarized exciton in vacuum at  $q = 0$ , Eq. (1). The overall vacuum benchmark results (1) are shown with the dash-dotted lines. The total decay width is displayed by thick solid lines, the dashed solid lines (when distinguishable) show the part of the width due to the decay into vacuum photons only. The vertical dash lines indicate the position of the surface plasmon wave vector,  $\kappa_p/k$ , Eq. (4).

coherent effects as it is the interaction of many molecular transition dipoles (and their images) that would determine the properties of the excitation. Philpott,<sup>6</sup> for instance, pointed out that by placing a linear chain near a transparent substrate, one could probe some of otherwise non-radiant polariton states via emission of bulk substrate photons. It was also studied how the radiative decay properties of quantum wire excitons get modified when the wire is embedded in a microcavity, that is, via emission of cavity photons (Refs. 8,15 and references quoted there). As one-dimensional arrays are considered for the directed energy transfer applications, their interaction with the environment may also be used to achieve certain purposes such as, e.g., to counteract losses by embedding the array in the gain medium.<sup>16</sup>

In this paper we discuss 1D coherent dipole excitations that are formed in the neighborhood of the planar reflecting substrate in the range of frequencies  $\omega$  where the dielectric constant of the substrate medium  $\epsilon(\omega) < 0$  and the substrate does not support bulk photon modes. This is the situation that is most easily implementable in the vicinity of a metallic surface and which, in fact, has recently received a considerable attention in the context of both organic excitons<sup>17</sup> and dipole excitations of nanoparticles (Ref. 18 and references therein). The sub-

strate in general affects both the dispersion of the excitons and their life-time. We will show that the presence of the substrate may result in new interference patterns and leads to a plethora of behaviors depending on the polarization and frequency of the excitation as well as on the distance from the interface. For the decay width, this is illustrated in Fig. 1 that exemplifies substantial differences with the vacuum result (1) and is discussed in more detail later. This Figure demonstrates not only a modification of the exciton decay into vacuum photons but also the decay into substrate surface plasmon (SP) modes (that occur for  $\epsilon(\omega) < -1$ ), significance of the latter channel strongly increasing upon approach to the interface.

Importance of the coupling of an individual dipole excitation to substrate SP modes and of associated resonance decay and scattering phenomena have already been stressed both for molecules<sup>19,20,21</sup> and nanoparticles.<sup>18</sup> This coupling strongly increases as the exciton transition frequency approaches the “resonance” region of the substrate in which  $\epsilon(\omega)$  is close to  $-1$ . The increase is, of course, what should be expected from the theory of electrostatic image forces<sup>22</sup> which features the combination factor

$$Q_0 = (1 - \epsilon)/(1 + \epsilon) \quad (3)$$

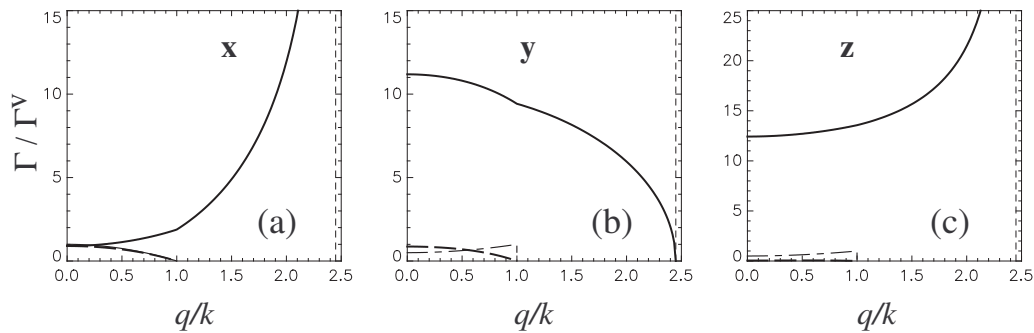


FIG. 2: As in Fig. 1 but for  $d = 50a$  and  $\epsilon = -1.2$ . Note that despite the separation distance here is 5 times larger than in panels (d-f) of Fig. 1, the decay into substrate surface plasmons is much stronger.

for the magnitude of image charges. One should be aware, however, that this is also the region where both retardation<sup>19,20</sup> and dissipation<sup>11</sup> effects are particularly important. The corresponding enhancement of the decay of 1D excitons into SPs is seen in the illustration of Fig. 2 ( $\epsilon = -1.2$ ) where, in comparison with Fig. 1 ( $\epsilon = -10$ ), it clearly is a dominant decay channel; consequently the fluorescence efficiency is greatly reduced.<sup>20</sup> One also appreciates the fact that the resonant enhancement, as shown, occurs over the already “super-radiant” vacuum decay rate.

Both Figs. 1 and 2 have been calculated with negligible exciton scattering and substrate losses (see Sec. IV for discussion of dissipation effects), hence they are reflective of the full conservation laws for our exciton-photon-SP system. So excitons with wave vectors  $|q| > k$  cannot decay into vacuum photons, while emission of SPs can occur only for  $|q| < \kappa_p(k)$  where

$$\kappa_p = k [\epsilon/(\epsilon + 1)]^{1/2} \quad (4)$$

is the well-known (e.g., Ref. 10) wave vector of the SP at an appropriate frequency. In such an idealized system, exciton-polaritons with larger wave vector magnitudes would be non-emissive. An example of the corresponding qualitative picture of the dispersion spectrum of exciton-polaritons in the chain is shown schematically in Fig. 3. The non-emissive branch 2 there can be thought of as of excitations representing a coherent mix of the exciton, photons and SPs of the same momentum projection along the chain, the relative weight contributions depending on this momentum. (The branch splitting exhibited in Fig. 3 would not take place for **y**-polarized excitons as consistent with the SP polarization.) We cannot exclude that surface plasmon guiding by chains of nanoparticles found in recent numerical simulations<sup>23</sup> is related to the formation of the discussed bound exciton-SP states.

As the SPs are surface states characterized by 2D wave vectors, the inverse square-root singular behavior in the decay rates of 1D excitons upon  $q \rightarrow \kappa_p$  seen in Figs. 1 and 2 has the “dimensionality” origin similar to the one taking place for 2D (quantum well) excitons decaying into 3D vacuum photons<sup>1,5,24,25</sup> and 1D (quantum wire) excitons decaying into 2D cavity photons.<sup>8</sup>

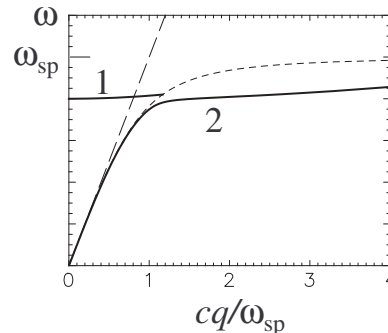


FIG. 3: Schematically (not to scale!), an example of the possible idealized dispersion of **x**-polarized 1D exciton-polaritons in the form of their frequency  $\omega = E(q)/\hbar$  as a function of the wave vector  $q$ . Here the exciton-polariton spectrum (solid lines) is split into two branches: the states of branch 1 decay via emission of photons and/or SPs, the states of branch 2 are non-emissive. This spectrum is a result of the interaction of the bare excitons with vacuum photons, whose spectrum is reflected in the limiting long-dash line, and with substrate surface plasmons, whose spectrum is reflected in the limiting short-dash line.  $\omega_{sp}$  is the asymptotic SP frequency.

In what follows we will elaborate on the interaction of 1D excitons with the neighboring reflecting substrate using the simplest model of a chain of molecules with a single molecular dipole transition (Frenkel-like excitons). We note that some resulting features would be generically valid for Wannier-Mott excitons as well. We however do not pursue here an explicit analysis of the Wannier-Mott excitons that would require specific modifications for their bare dispersion as well as the influence of the substrate on the exciton binding and oscillator strength. While we chose, for certainty, to use an example of the metallic substrate and the corresponding surface plasmon excitations, it should be clear that the same effects would occur for a dielectric substrate whenever it can feature the region of negative  $\epsilon(\omega)$  and the surface polariton excitations.

## II. FRENKEL EXCITON-POLARITONS IN A MOLECULAR CHAIN. VACUUM RESULTS.

Renormalization of a single-molecule transition of energy  $E_f$  and the formation of an electric-dipole exciton band in a molecular aggregate can be derived in various frameworks (see, e.g., Refs. 1,26) with identical results. Here we will use a simple and physically transparent description having a clear underlying semi-classical analogy. In the Heitler-London approximation (energy  $E_f$  is much larger than all other energies involved), the exciton Hamiltonian for interacting identical molecules can be written as

$$\begin{aligned} H &= (E_f + V_0) \sum_n B_n^\dagger B_n + \sum_{n>m} V_{n-m} (B_n^\dagger B_m + \text{h.c.}) \\ &= \sum_q E(q) B_q^\dagger B_q, \end{aligned}$$

where  $B_n^\dagger$  creates an excitation on the  $n$ th molecule whereas  $B_q^\dagger = N^{-1/2} \times \sum_n e^{iqna} B_n^\dagger$  creates an excitation of the wave vector  $q$  in a chain of  $N$  molecules with the intermolecular spacing  $a$ . Correspondingly, the exciton energy

$$E(q) = E_f + V_0 + 2 \sum_{n>0} V_n \cos(qna), \quad (5)$$

where  $V_0$  represents a possible renormalization for a single molecule<sup>31</sup> while  $V_n$  the *effective* intermolecular interaction as mediated by the electromagnetic field. The interaction is handily expressed via the semi-classical expression

$$V_n = -\mathbf{p} \cdot \mathbf{E}(na\hat{\mathbf{x}}), \quad (6)$$

with  $\mathbf{p}$  being the molecular transition dipole moment and  $\mathbf{E}(na\hat{\mathbf{x}})$  the electric field produced by the dipole  $\mathbf{p} = p\hat{\mathbf{p}}$  at the distance  $na$  along the chain axis chosen to be along  $x$  (we use caps to denote unit vectors).

If the electric field  $\mathbf{E}$  is the total retarded field, however, it is in fact also a function of the oscillating dipole frequency  $\omega = ck$  and has both real and imaginary parts. Equation (5) then has to be rewritten as a more general equation

$$E(q) = E' - i\Gamma/2 = E_f + \Sigma(k, q), \quad (7)$$

involving the self-energy correction  $\Sigma(k, q)$ , the real-space transform of which

$$\Sigma(k, x) = -\mathbf{p} \cdot \mathbf{E}(k, x\hat{\mathbf{x}}) \quad (8)$$

serves to replace (6). Equation (7) self-consistently (via  $k = E/\hbar c$ ) determines both the dispersion  $E'(q) = E_f + \text{Re}\{\Sigma(k, q)\}$  and the decay width  $\Gamma(q) = -2\text{Im}\{\Sigma(k, q)\}$  of the exciton-polariton states as a function of their wave vector  $q$ . This simple approach, alternatively formulated in terms of Green's functions, is both physically appealing and powerful as it involves only classically calculable

electric fields; various aspects of it have been used for different geometries (e.g., Refs. 10,11,14 and references therein). In this paper we will not pursue solving specific self-consistent problems that may depend on a multitude of parameters and, instead, be discussing the self-energy for a given *real* value of parameter  $k$  (that is, the oscillating frequency) for different values of the excitation wave vector  $q$ . For our numerical illustrations in this paper we chose a representative value of  $k$  corresponding to the wavelength  $\lambda = 2\pi/k = 400a$ , a reasonable magnitude for the optical region of the spectrum given typical spacing  $a \sim 10 \text{ \AA}$ . Understandably, typical values for nanoparticle systems would be different.<sup>4</sup> If neglecting the retardation effects (purely electrostatic fields), the value of  $k$  would have to be set equal to zero.

Let us briefly review the application to a molecular chain in vacuum (see also Refs. 6 and 4). Consider the standard<sup>22</sup> retarded electric field at the point  $\mathbf{r} = r\hat{\mathbf{r}}$  from the oscillating point dipole in vacuum:

$$\begin{aligned} \mathbf{E}^v(k, \mathbf{r}) &= \frac{e^{ikr}}{r} \left\{ k^2 [\mathbf{p} - \hat{\mathbf{r}}(\hat{\mathbf{r}} \cdot \mathbf{p})] \right. \\ &\quad \left. + \left( \frac{1}{r^2} - \frac{ik}{r} \right) [3\hat{\mathbf{r}}(\hat{\mathbf{r}} \cdot \mathbf{p}) - \mathbf{p}] \right\} \quad (9) \end{aligned}$$

and the corresponding

$$\Sigma^v(k, \mathbf{r}) = -\mathbf{p} \cdot \mathbf{E}^v(k, \mathbf{r}).$$

This expression turns out to be directly applicable even for the decay of a single molecule (see also Ref. 10): indeed, calculating  $-2\text{Im}\{\Sigma^v(k, \mathbf{r} \rightarrow 0)\}$  immediately leads to the well-known decay width (2). To derive the decay rate for a 1D exciton state with wave vector  $q$ , one augments this decay by the sum of contributions from other molecules:

$$\Gamma^v(k, q) = \Gamma^0(k) - 4 \sum_{n>0} \cos(qna) \text{Im}\{\Sigma^v(k, na\hat{\mathbf{x}})\}$$

resulting, after evaluation of the sum, in already quoted Eq. (1). Exemplifying a general feature of self-energy corrections, a direct inspection easily verifies that, for a fixed  $k$ , Eqs. (1) and (2) satisfy, as expected,

$$\sum_q \Gamma^v(k, q) = N \Gamma^0(k). \quad (10)$$

With the real part of the field (9), one immediately obtains the effective resonant interaction matrix element:

$$\begin{aligned} \frac{1}{p^2} \text{Re}\{\Sigma^v(k, x)\} &= (1 - 3\cos^2\theta) \left[ \frac{\cos(kx)}{x^3} + \frac{k \sin(kx)}{x^2} \right] \\ &\quad - (1 - \cos^2\theta) \frac{k^2 \cos(kx)}{x}, \quad (11) \end{aligned}$$

exactly the same result that would be derived in the picture of the virtual photon exchange.<sup>26</sup> Calculating the corresponding sums with  $n > 0$  (and disregarding the irrelevant single-molecule renormalization<sup>31</sup>) for many

molecules in the long wavelength,  $qa \ll 1$ , expansion, one arrives at

$$\frac{a}{p^2} \text{Re}\{\Sigma^v(k, q)\} \simeq \frac{(1 - 3\cos^2\theta)}{2} \left[ \frac{4\zeta(3)}{a^2} + k^2 - 3q^2 - (k^2 - q^2)b \right] + (1 - \cos^2\theta) k^2 b, \quad (12)$$

where  $\zeta(3) \simeq 1.202$  and  $b = \ln(|k^2 - q^2|a^2)$ . (It is useful to note that approximation (12) actually works very well over a sizable portion of the exciton Brillouin zone.) The known logarithmic divergence in Eq. (12) upon  $q \rightarrow k$  signifies the splitting of the exciton-polariton spectrum into two branches<sup>5,6,7</sup> as caused by the radiative zone component of the field at  $\cos\theta \neq 1$  in Eq. (11). Of course, corresponding to this divergence there is a non-vanishing decay rate at  $q \rightarrow k$  in Eq. 1. The vanishing of the latter takes place only at  $\cos\theta = 1$ , and in this case the exciton dispersion exhibits a single-branch behavior with a cusp at  $q = k$ .

The electrostatic part of Eq. (12) features a non-analytic behavior  $\propto q^2 \ln(qa)^2$  at  $|q| \gg k$  due to the long-range nature of the dipole-dipole interaction making the exciton dispersion “steeper”, the behavior that recently attracted attention in the context of exchange-interaction effects for excitons in carbon nanotubes.<sup>27</sup> The overall width of the bare exciton zone as seen in Eq. (12) is scaled with the energetic parameter

$$J = p^2/a^3 \quad (13)$$

establishing the unit for the nearest-neighbor electrostatic dipole-dipole interaction. To appreciate the scale of energies involved: with  $p = 1$  Debye and  $a = 10 \text{ \AA}$ , for instance,  $J \simeq 0.014 \text{ eV}$ . With reasonable variations of values of  $p$  and  $a$ ,  $J$  could reach magnitudes  $\sim 0.1 \text{ eV}$ .

### III. MOLECULAR CHAIN NEAR THE INTERFACE.

In the vicinity of the interface with a metallic/dielectric body, the total electric field can be conveniently represented as a sum of the primary, vacuum, field, discussed in section II, and the secondary field due to the induced response of that body:  $\mathbf{E} = \mathbf{E}^v + \mathbf{E}^s$ . Correspondingly, the self-energy of the exciton-polaritons is also represented as  $\Sigma = \Sigma^v + \Sigma^s$ . In what follows we discuss the induced contribution  $\Sigma^s(k, q)$  coming from a half-space characterized by the dielectric constant  $\epsilon = \epsilon(\omega)$  taken at the frequency  $\omega = ck$  in the geometry of the molecular chain (along  $\mathbf{x}$ ) being parallel to the separating interface ( $xy$ -plane) at the distance  $z_0 = d/2$  from it ( $d$  is the distance between a dipole and its image).

The problem of an electric dipole near a metallic/dielectric half-space is a classical problem first treated by Sommerfeld<sup>10,28</sup> and whose solution is available in different forms. Here we find it convenient to adopt the expressions for the electric field as derived in Ref. 29. In the context of our application for fields along the chain,

it matters how the dipoles are oriented with respect to both the chain and the interface. For a chain of electric dipoles of an arbitrary polarization  $\hat{\mathbf{p}}$ , one easily finds that

$$\Sigma^s(k, x) = \hat{p}_x^2 \Sigma_{\mathbf{x}}^s(k, x) + \hat{p}_y^2 \Sigma_{\mathbf{y}}^s(k, x) + \hat{p}_z^2 \Sigma_{\mathbf{z}}^s(k, x),$$

where axes-related components can be rewritten from results in Ref. 29 as follows:

$$\frac{1}{p^2} \Sigma_{\mathbf{x}}^s(k, x) = \int_0^\infty \kappa d\kappa e^{-\gamma d} \left( \frac{\gamma Q}{2} J_-(\kappa x) + \frac{k^2 P}{2\gamma} J_+(\kappa x) \right) \quad (14)$$

for  $\mathbf{x}$ -polarized dipoles,

$$\frac{1}{p^2} \Sigma_{\mathbf{y}}^s(k, x) = \int_0^\infty \kappa d\kappa e^{-\gamma d} \left( \frac{\gamma Q}{2} J_+(\kappa x) + \frac{k^2 P}{2\gamma} J_-(\kappa x) \right) \quad (15)$$

for  $\mathbf{y}$ -polarized dipoles, and

$$\frac{1}{p^2} \Sigma_{\mathbf{z}}^s(k, x) = \int_0^\infty \kappa d\kappa e^{-\gamma d} \frac{\kappa^2 Q}{\gamma} J_0(\kappa x) \quad (16)$$

for  $\mathbf{z}$ -polarized dipoles. In Eqs.(14-16),

$$J_{\pm}(x) = J_0(x) \pm J_2(x)$$

are composed of Bessel functions of the first order while parameters

$$Q = \frac{\gamma_\epsilon - \epsilon\gamma}{\gamma_\epsilon + \epsilon\gamma}, \quad P = \frac{\gamma_\epsilon - \gamma}{\gamma_\epsilon + \gamma} \quad (17)$$

and

$$\gamma = (\kappa^2 - k^2)^{1/2}, \quad \gamma_\epsilon = (\kappa^2 - \epsilon k^2)^{1/2} \quad (18)$$

(for negative  $u < 0$ ,  $u^{1/2} = -i(-u)^{1/2}$  should be used in Eq. (18).) One can straightforwardly verify that the no-retardation limit ( $k = 0$ ) of the above expressions leads to usual electrostatic fields of image dipoles.

Representations (14-16) are quite meaningful physically. One immediately observes that the pole in the parameter  $Q$  in (17) occurs at  $\kappa$  equal to  $\kappa_p$  in Eq. (4), the wave vector of the surface plasmon (surface polariton) whenever real  $\epsilon < -1$ . Together with  $p$ -polarized photons, SPs make the  $Q$ -containing contributions in Eqs. (14-16). The parameter  $P$ -containing terms, on the other hand, correspond to contributions to the electric fields from  $s$ -polarized photons. Expressions (14-16) taken at the source point  $x = 0$  would describe the effect of the half-space on the electronic transition in a single molecule as studied in Refs. 19,20.

We now turn to the  $q$ -dependent self-energy of an exciton in a long chain of molecules. Restricting to the chain-to-interface distances larger than the intermolecular spacing:  $d \gg a$ , one can safely use a continuum description of the half-space response:

$$\Sigma^s(k, q) = 2 \int_0^\infty \frac{dx}{a} \Sigma^s(k, x) \cos(qx). \quad (19)$$

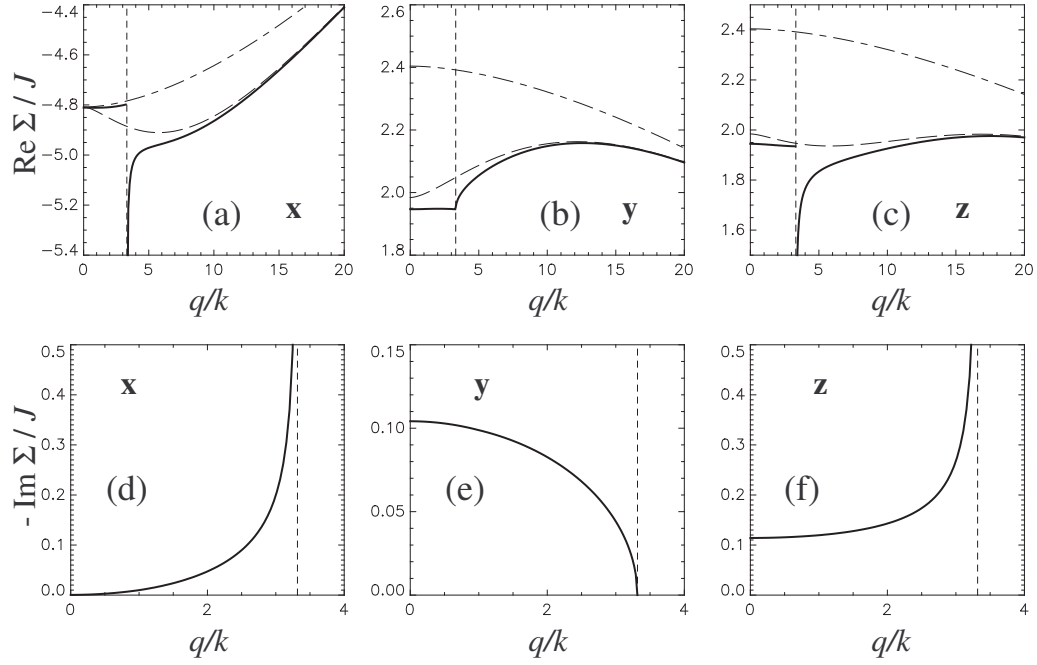


FIG. 4: Real (upper panels) and imaginary (lower panels) of the self-energy  $\Sigma(k, q)$  of exciton-polaritons as functions of the reduced wave vector  $q/k$  for a fixed value of  $k = 2\pi/400 a$ ,  $\epsilon = -1.1$  and  $d = 10a$ . Self-energy is shown with respect to  $J$  from Eq. (13). The vertical short-dash lines show the position of the surface plasmon wave vector,  $\kappa_p/k$ . In the upper panels, the long-dash lines show the electrostatic (no-retardation) results, dash-dotted lines the electrostatic results for the exciton dispersion in vacuum.

As with the vacuum case, all results are clearly even functions of  $q$ ; to simplify expressions, we will therefore continue assuming  $q > 0$ . Transformation (19) for individual dipole contributions (14-16) is facilitated by the integrals:<sup>30</sup>

$$\int_0^\infty dx \cos(qx) J_0(\kappa x) = \frac{1}{(\kappa^2 - q^2)^{1/2}} \Theta(\kappa - q), \quad (20)$$

$$\int_0^\infty dx \cos(qx) J_2(\kappa x) = \frac{1 - 2q^2/\kappa^2}{(\kappa^2 - q^2)^{1/2}} \Theta(\kappa - q) \quad (21)$$

so that Eq. (16), e.g., is transformed into

$$\frac{a}{p^2} \Sigma_{\mathbf{z}}^s(k, q) = 2 \int_q^\infty \frac{\kappa^3 Q e^{-\gamma d}}{\gamma(\kappa^2 - q^2)^{1/2}} d\kappa \quad (22)$$

and similarly for Eqs. (14) and (15). Step-functions in Eqs. (20) and (21), as is also reflected in Eq. (22), have a clear physical significance of the energy-and-momentum conservation limitation.

It is also useful and meaningful to note the no-retardation limit ( $k = 0$ ) of the above expressions, when  $Q$  in Eq. (17) becomes equal to the electrostatic combination (3), and the exciton dispersion would be affected by the image dipoles as

$$\frac{a}{Q_0 p^2} \Sigma_{\mathbf{x}}^s(q) = 2q^2 \int_q^\infty \frac{e^{-\kappa d}}{(\kappa^2 - q^2)^{1/2}} d\kappa = 2q^2 K_0(qd), \quad (23)$$

$$\frac{a}{Q_0 p^2} \Sigma_{\mathbf{y}}^s(q) = 2 \int_q^\infty (\kappa^2 - q^2)^{1/2} e^{-\kappa d} d\kappa = \frac{2q}{d} K_1(qd), \quad (24)$$

and

$$\Sigma_{\mathbf{z}}^s(q) = \Sigma_{\mathbf{x}}^s(q) + \Sigma_{\mathbf{y}}^s(q), \quad (25)$$

where  $K_0(x)$  and  $K_1(x)$  are the modified Bessel functions.

The effects of these real image corrections are displayed in Fig. 4 showing an example of the total  $q$ -dependent exciton self-energy  $\Sigma(k, q)$  including both vacuum and secondary field contributions. The figure is a result of an illustrative calculation for an idealized (no dissipation) system in the resonance region ( $\epsilon = -1.1$  so that  $\kappa_p \simeq 3.3k$ ) at a relatively close ( $d = 10a$ ) distance from the interface – to demonstrate a possible magnitude of the effects. The figure shows both the retardation effects as well as the fact that upon the increase of the wave vector  $q$ , the exciton dispersion approaches the electrostatic behavior. It is clear that, in principle, the electrostatic image forces may appreciably modify the exciton dispersion.

In an idealized system, the secondary field contributions to the imaginary part of the self-energy (exciton decay) can come only from two sources. First, it is the regions of variable  $\kappa$  in the integrals where the parameter  $\gamma$  (18) is imaginary. As Eq. (22) shows, that happens only for  $q < k$  – this is the source of the modification by the substrate of the exciton decay into vacuum photons that

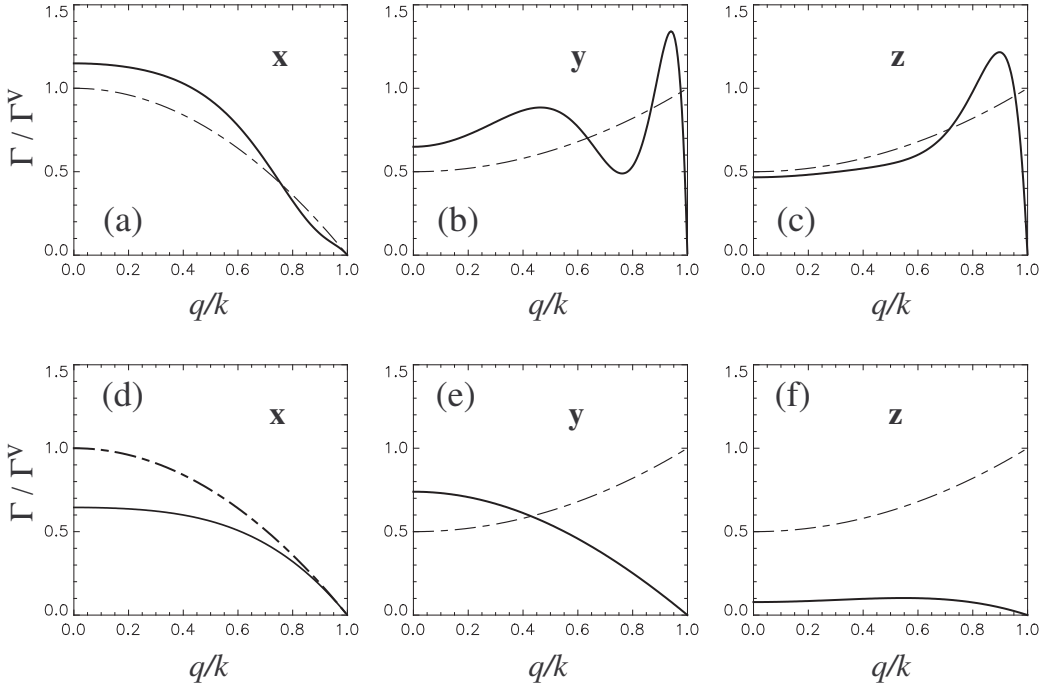


FIG. 5: Decay width  $\Gamma(k, q)$  of the exciton-polariton as a function of the reduced wave vector  $q/k$  for a fixed value of  $k$  and  $\epsilon = -0.8$ . Two rows correspond to different dipole-to-image-dipole distances: upper panels (a–c) are for  $d = 600a$ , lower panels (d–f) for  $d = 10a$ . There is no surface plasmon channel here, and the total decay width is due to the vacuum photons only.

we explicitly illustrated in Fig. 1. Second, and dominating in Fig. 4, source is the surface plasmon pole  $\kappa = \kappa_p$  in the parameter  $Q$  in the integrals. As Eq. (22) shows again, this pole contributes only for  $q < \kappa_p$  signifying the decay of the exciton into a SP. The pole contributions to  $-\text{Im}\{\Sigma(k, q)\}$  are immediately calculable and can be represented by a combination of a common factor

$$\frac{4\pi}{|\epsilon|^{1/2}(1-\epsilon)} \frac{p^2 \kappa_p^4}{ak^2} \exp\left[-d(\kappa_p^2 - k^2)^{1/2}\right] \quad (26)$$

and polarization- and  $q$ -dependent co-factors:

$$q^2/\kappa_p(\kappa_p^2 - q^2)^{1/2} \quad (27)$$

for  $\mathbf{x}$  polarization,

$$(\kappa_p^2 - q^2)^{1/2}/\kappa_p \quad (28)$$

for  $\mathbf{y}$  and

$$|\epsilon| \kappa_p/(\kappa_p^2 - q^2)^{1/2} \quad (29)$$

for  $\mathbf{z}$ .

Accompanying decay's inverse square-root singularity in Eqs. (27) and (29), also seen in Fig. 4(d) and (f), are the diverging discontinuities in the real parts (panels (a) and (c) of Fig. 4) of the type familiar from the studies of the decay of 2D excitons into 3D vacuum photons.<sup>1,5,24,25</sup> Due to such a discontinuity, the resulting self-consistent dispersion of, e.g.,  $\mathbf{x}$ -polarized excitations would split into two branches as shown in Fig. 3. On the contrary,

the decay rate of  $\mathbf{y}$ -polarized excitons vanishes at  $q \rightarrow \kappa_p$  in Eq. (28). This is a consequence of the polarization of SPs whose electric field can have only longitudinal and perpendicular to the interface components (like  $p$ -polarized photons). As  $q \rightarrow \kappa_p$ , the surface plasmons would be emitted along the chain direction, hence their field would have no  $\mathbf{y}$ -components to interact with  $\mathbf{y}$ -excitons. (There is a similarity here with the decay of  $\mathbf{x}$ -polarized excitons in vacuum, whose decay rate vanishes at  $q \rightarrow k$ , Eq. (1).) Correspondingly, the real part of the self-energy in Fig. 4(b) does not exhibit a discontinuity at  $q = \kappa_p$  (the discontinuity is in the derivative) with the resulting exciton spectrum consisting of one branch only. Quite clear is also  $\propto q^2$  behavior for  $\mathbf{x}$ -excitons in Eq. (27), it has the same origin as in the electrostatic effect (23) – at  $q \rightarrow 0$ , the exciton polarization of the chain becomes uniform and there would be no polarization charges (a vanishing spatial derivative) to induce images in the substrate.

The SP excitations in the substrate exist in the region of frequencies where  $\epsilon(\omega) < -1$ . Qualitatively different, therefore, for a reflecting substrate is another region of frequencies in which  $-1 < \epsilon(\omega) < 0$ . In this case exciton-polaritons in the molecular chain can decay only into vacuum photons. The (idealized) substrate then serves as to modify the dispersion of excitons and their radiative decay. An example of the radiative decay modification is shown in Fig. 5 calculated for  $\epsilon = -0.8$  and to be compared with Fig. 1. Both figures feature the same distances from the interface but different magni-

tudes *and* signs of the image charges, Eq. (3). These two facts explain similarities and differences in the radiative decay patterns for the two examples. Among the important common features, one should notice “oscillating”  $q$ -dependences of the decay rate at larger distances and the vanishing of the radiative decay at  $q \rightarrow k$ . As the chain is moved further away from the interface, even more undulations would be observed in the  $q$ -dependence of the decay rate as a result of the interference with the image dipoles.

#### IV. EFFECTS OF DISSIPATION IN THE SUBSTRATE

Real metallic (dielectric) substrates are characterized by finite dissipation (losses) that are taken into account phenomenologically via the imaginary part of the dielectric function:

$$\epsilon(\omega) = \epsilon'(\omega) + i\epsilon''(\omega).$$

In the context of the effects of  $\epsilon''$  on SPs, for a given real frequency  $\omega$ , wave vectors of the SPs consequently acquire imaginary parts as well:<sup>10</sup>

$$\kappa_p = \kappa'_p + i\kappa''_p,$$

where  $\kappa''_p$  describes the damping of the SP modes. Another way to look at  $\kappa''_p$  is as of the uncertainty (broadening) of the SP’s wave vector. Hence the momentum conservation law in the exciton decay into a SP would not be obeyed exactly as in idealized systems discussed so far. One thus should expect a broadening and extension of the range of finite exciton decay rates into the region of the exciton wave vectors  $q > \kappa'_p$ . Moreover, even with *relatively* small losses,  $\epsilon'' \ll |\epsilon'|$ , the relative damping of the SP can become substantial in the resonance region of  $\epsilon'$  close to  $-1$ . Indeed, in this case<sup>10</sup>

$$\kappa''_p/\kappa'_p \simeq \frac{\epsilon''/\epsilon'}{2(\epsilon' + 1)}, \quad (30)$$

and the denominator in the r. h. s. of Eq. (30) could “compensate” for the smallness of  $\epsilon''$  and completely destroy the notion of a coherent SP.

Figure 6 shows results of the calculation of the exciton decay for the substrate with the dielectric constant  $\epsilon = -1.2 + 0.05i$  and variable distances to the interface. As compared to the idealized system, one immediately notices very broad, especially at smaller distances,  $q \gg \kappa'_p$  regions of the exciton decay. For this particular value of the complex dielectric function, however, the “uncertainty” ratio (30) is only about 0.1. Thus the extremely broadened  $q$ -region of the exciton decay is not due to the broadening of the SPs themselves, the latter can explain only the formation of the finite magnitude SP peaks clearly seen in Fig. 6. Of course, with complex dielectric constants, the imaginary part of the exciton self-energy discussed in Sec. III is contributed to, in principle,

by the whole integration range in integrals like Eq. (22), rather than just by the around-the-pole region. What is reflected in the broad “wings” in Fig. 6 is the result of the ordinary “incoherent” Joule losses due to the oscillating electric field of the exciton polarization penetrating into the substrate. Especially illuminating in this regard is a second maximum on the top-most curve in Fig. 6(a). Indeed, similarly to the already discussed in Sec. III image-charge effects, the electrostatic component of the electric field of  $\mathbf{x}$ -polarized excitons has a  $q$ - and  $d$ -dependence reflected in the r. h. s. of Eq. (23), the maximum of which is achieved at  $q \sim 1/d$ . As the distance from the interface increases, the role of such short-range energy transfer from the higher- $q$  excitons to the substrate decreases and one can “tune” it off while still having an appreciable decay rate of the lower- $q$  states into SPs. In addition to the largest-distance curves in Fig. 6, this point is illustrated in Fig. 7 showing clear SP emission effects both close to and away from the resonance region. The distance dependence of the SP emission intensity is governed by the factor (26) and one could likely “optimize” the relationship between the coherent and incoherent energy transfer based on the system regime parameters.

#### V. DISCUSSION.

The modification of the electric fields in the presence of the reflecting substrate leads to substantial changes of the properties of 1D exciton-polaritons in a dipole-coupled chain above the substrate. The substrate modifies the interaction of the exciton with vacuum photons and, in addition, can engage a new and efficient interaction channel – with surface excitations of the substrate. While these statements also apply to a well-studied<sup>19,20</sup> case of a single molecule near the interface, the cooperative interaction of many molecules in the chain and of their images may lead to qualitatively and quantitatively interesting effects. In this paper, we discussed such effects for coherent delocalized 1D exciton-polaritons that are well characterized by their wave vectors  $q$ . We emphasize that it is actually individual  $q$ -states that would exhibit qualitatively different coherent properties – if averaged uniformly over all  $q$ , a (near) reduction would occur to the effects of the substrate on an individual molecule (similarly to discussed Eq. (10) for vacuum). Immediately noticeable in our illustrative examples, for instance, is a difference of the behavior of  $\mathbf{x}$ - and  $\mathbf{y}$ -polarized 1D exciton-polaritons – while those cases of the molecular transition dipoles parallel to the interface would be equivalent for single molecules. Properties of 1D exciton-polaritons depend specifically on their polarization, frequency with respect to the substrate dielectric dispersion and distance from the interface. We reiterate that, while our illustrations used parameters appropriate for molecular systems, qualitatively similar effects are expected for other systems such as chains of nanoparticles.

A common feature for all exciton polarizations and

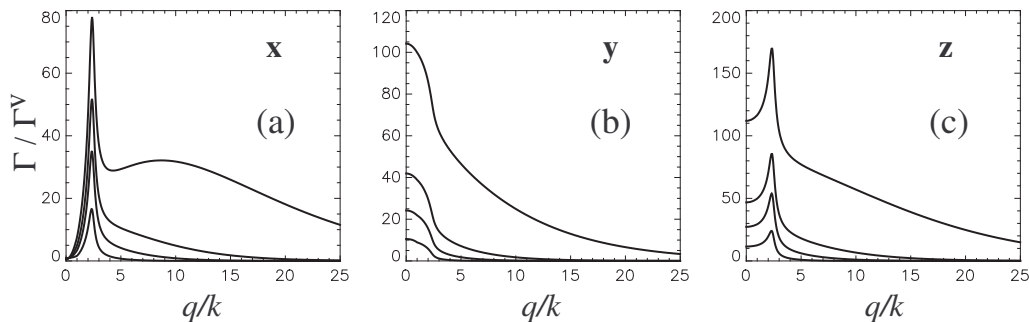


FIG. 6: Decay width  $\Gamma(k, q)$  of exciton-polaritons as a function of the reduced wave vector  $q/k$  for a fixed value of  $k = 2\pi/400 a$  in units of vacuum  $\Gamma^v = 2\pi p^2 k^2/a$  and for different (indicated in the panels) exciton polarizations. Here substrate's dielectric constant is *complex*:  $\epsilon = -1.2 + 0.05i$ . Each of the panels contain 4 curves corresponding to different distances between the molecular chain and the substrate (top to bottom):  $d = 10 a, 20 a, 30 a$  and  $50 a$ .

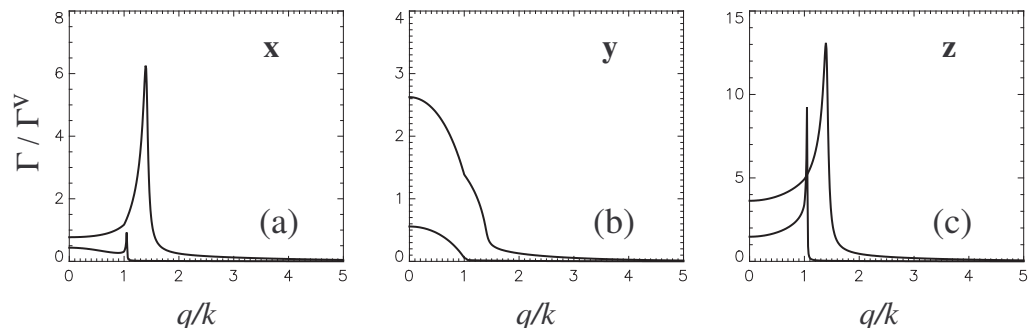


FIG. 7: As in Fig. 6 but for  $d = 50 a$  and two different dielectric functions (top to bottom):  $\epsilon = -2.0 + 0.1i$  and  $\epsilon = -10.0 + 0.5i$ .

conditions considered (see Figs. 1, 2, 5) is that the rate of the radiative decay into vacuum photons in the presence of the substrate vanishes at  $q = k = \omega/c$ , that is, where the exciton dispersion curve would cross the vacuum photon dispersion line (see, e.g., Fig. 3) – this is distinctly different from the case of the chain in the vacuum where such vanishing would occur only for excitons polarized parallel to the chain. The consequence of this effect of the image dipoles is that no branch splitting occurs at  $q = k$ . At distances from the interface comparable to the wavelength  $2\pi/k$  of vacuum photons, the interference with the radiative fields of the image dipoles results in undulated patterns of the radiative decay (panels (a-c) of Figs. 1, 5) as functions of  $q$ ; the larger the distance the more undulations would take place.

It is important to note that, as a result of integration (19) over many molecules in the chain, the magnitudes of these and some other  $q$ -dependent features fall off with the distance from the interface slower than their averages characteristic of single molecules. Consider, e.g., the electrostatic exciton energy shifts due the interaction of the molecular dipole(s) with their image(s). For a single molecule, the corresponding transition energy shift is  $\sim p^2/d^3$ . The maximum of  $q$ -dependent shifts, however, as Eqs. (23-25) show, would be  $\sim p^2/ad^2$  – that is, much larger at distances  $d \gg a$  (not in the immediate proximity of the interface). This may provide an opportunity of

easier experimental identification of such shifts than for individual molecules.

While the distance dependence (26) of the decay rate of the excitons into surface plasmons is the same as for single molecules,  $q$ -dependent enhancing factors (27) and (29), seen as the peaks in our illustrations, may facilitate better experimental verifications. As the rate of the emission of SPs is  $q$ -dependent, we speculate that the chain excitons could perhaps serve as directional sources of SPs – in expectation of a more efficient emission along the chain for  $x$ - and  $z$ -polarized excitons and perpendicular to the chain for  $y$ -polarized excitons. We recall that these polarization assignments stem from the fact that the electric field of the SPs lies in the plane made by the wave vector and the normal to the interface. As the small- $q$  exciton decay into SPs can be strongly enhanced in comparison with the decay into vacuum photons, it is likely that the inverse process of the excitation of the chain by SPs could also be exploited. Non-emissive exciton-polaritons with larger  $q$  may also present an opportunity to be used for SP guiding.<sup>23</sup>

Various scattering and dissipation processes are known to be able to strongly affect features characteristic of idealized systems. We particularly discussed the chain exciton quenching due to the “incoherent” energy transfer to the substrate – and this does not exhaust the list. It suffices to also mention, e.g., the scattering by phonons in

molecular chains or Joule losses in the chains of metallic nanoparticles. The fast scattering between different  $q$ -states would result in the thermalized population of the exciton-polaritons so that observed decay rates are thermally averaged (see Refs. 7, 9, 27 for some specific 1D applications). We therefore presume that the best conditions to experimentally address finer  $q$ -dependent effects we discussed in this paper would be low-temperature spectroscopic measurements.

## Acknowledgments

We gratefully acknowledge support from AFOSR grant FA 9550-05-1-0409 and from the Collaborative U. T. Dallas–SPRING Research and Nanotechnology Transfer Program. VMA also thanks Russian Foundation of Basic Research and Ministry of Science and Technology of Russian Federation.

- 
- <sup>1</sup> V. M. Agranovich, *Theory of Excitons* (Nauka, Moscow, 1968), updated English language edition is in preparation by Oxford University Press.
- <sup>2</sup> F. Dubin, R. Melet, T. Barisien, R. Grousson, L. Legrand, M. Schott, and V. Voliotis, *Nature Physics* **2**, 32 (2006).
- <sup>3</sup> H. Bässler, *Nature Physics* **2**, 15 (2006).
- <sup>4</sup> V. A. Markel and A. K. Sarychev, *Phys. Rev. B* **75**, 085426 (2007).
- <sup>5</sup> V. M. Agranovich and O. A. Dubovsky, *JETP Lett.* **3**, 223 (1966).
- <sup>6</sup> M. R. Philpott, *J. Chem. Phys.* **63**, 485 (1975).
- <sup>7</sup> D. S. Citrin, *Phys. Rev. Lett.* **69**, 3393 (1992).
- <sup>8</sup> Y. N. Chen and D. S. Chuu, *Europhys. Lett.* **54**, 366 (2001).
- <sup>9</sup> C. D. Spataru, S. Ismail-Beigi, R. B. Capaz, and S. G. Louie, *Phys. Rev. Lett.* **95**, 247402 (2005).
- <sup>10</sup> L. Novotny and B. Hecht, *Principles of Nano-Optics* (Cambridge University Press, Cambridge, 2006).
- <sup>11</sup> R. R. Chance, A. Prock, and R. Silbey, *Adv. Chem. Phys.* **37**, 1 (1978).
- <sup>12</sup> M. Cho and R. J. Silbey, *Chem. Phys. Lett.* **242**, 291 (1995).
- <sup>13</sup> H. R. Stuart and D. G. Hall, *Phys. Rev. Lett.* **80**, 5663 (1998).
- <sup>14</sup> R. L. Hartman and P. T. Leung, *Phys. Rev. B* **64**, 193308 (2001).
- <sup>15</sup> Y. N. Chen, D. S. Chuu, T. Brandes, and B. Kramer, *Phys. Rev. B* **64**, 125307 (2001).
- <sup>16</sup> D. S. Citrin, *Optics Lett.* **31**, 98 (2006).
- <sup>17</sup> J. Bellessa, C. Bonnand, and J. C. Plenet, *Phys. Rev. Lett.* **93**, 036402 (2004).
- <sup>18</sup> T. Søndergaard and S. I. Bozhevolnyi, *Phys. Rev. B* **69**, 045422 (2004).
- <sup>19</sup> H. Morawitz and M. R. Philpott, *Phys. Rev. B* **10**, 4863 (1974).
- <sup>20</sup> M. R. Philpott, *J. Chem. Phys.* **62**, 1812 (1975).
- <sup>21</sup> W. H. Weber and C. F. Eagen, *Optics Lett.* **4**, 236 (1979).
- <sup>22</sup> J. D. Jackson, *Classical Electrodynamics* (Wiley, New York, 1975).
- <sup>23</sup> A. B. Evlyukhin and S. I. Bozhevolnyi, *Laser Phys. Lett.* **3**, 396 (2006).
- <sup>24</sup> L. C. Andreani and F. Bassani, *Phys. Rev. B* **41**, 7536 (1990).
- <sup>25</sup> S. Jorda, U. Rössler, and D. Broido, *Phys. Rev. B* **48**, 1669 (1993).
- <sup>26</sup> D. P. Craig and T. Thirunamachandran, *Molecular Quantum Electrodynamics* (Academic Press, London, 1984).
- <sup>27</sup> V. Perebeinos, J. Tersoff, and P. Avouris, *Nano Letters* **5**, 2495 (2005).
- <sup>28</sup> A. Sommerfeld, *Partial Differential Equations in Physics* (Cambridge University Press, Cambridge, 2006).
- <sup>29</sup> R. W. P. King and G. S. Smith, *Antennas in Matter* (MIT Press, Cambridge, MA, 1981).
- <sup>30</sup> A. P. Prudnikov, Y. A. Brychkov, and O. I. Marichev, *Integrals and Series. Special Functions*. (OPA, Amsterdam, 1990).
- <sup>31</sup> Single molecule renormalization is, to a large extent, not important for our interests in this paper and we refer the reader to numerous studies dedicated to it. We will completely disregard the vacuum real energy shift of a single molecule which can be thought of as absorbed in  $E_f$ .